Reaction Chemistry & Engineering

ROYAL SOCIETY OF CHEMISTRY

PAPER

View Article Online
View Journal | View Issue

Cite this: *React. Chem. Eng.*, 2024, **9**, 108

Pyrolysis of biogas for carbon capture and carbon dioxide-free production of hydrogen†

Ahmet Çelik, Iadh Ben Othman, Heinz Müller,
Patrick Lott * and Olaf Deutschmann

Methane pyrolysis is considered an auspicious approach for large-scale hydrogen production and simultaneous carbon capture, hereby contributing to a decarbonization of the chemical industry. While commonly pure methane or natural gas serve as a feedstock, the usage of biogas may allow exploitation of the pyrolysis process as a carbon sink. In this context, the present study reports on biogas pyrolysis in a high-temperature reactor at temperatures between 1000 °C and 1600 °C, residence times between 1 s and 7 s, and molar $CH_4 : CO_2$ ratios in the biogas between 1 : 1 and 4 : 1. Among these conditions, high residence times, a high CH_4 content, and the introduction of a carbonaceous fixed bed in the reactor benefit high educt conversion, H_2 selectivity, and solid carbon yield. A carbon fixation of up to 95% was achieved during reference measurements with pure CH_4 feeds, whereas a carbon yield of 75% was found for biogas feeds. The analysis of the reaction product distribution uncovered a consumption of CO_2 *via* dry reforming, water gas shift, and Boudouard reactions, resulting in a maximum $H_2 : CO$ ratio of 3 : 1 in the effluent gas stream. Herewith, the study underscores that optimized reactor operation parameters allow for maximizing CH_4 and CO_2 conversion as well as for achieving $H_2 : CO$ ratios that are viable for further industrial applications, along with an efficient deposition of solid carbon.

Received 28th June 2023,
Accepted 12th September 2023

DOI: 10.1039/d3re00360d

rsc.li/reaction-engineering

Introduction

The goals defined in the Paris agreement to limit global warming are linked to a drastic reduction in greenhouse gas emissions[1] and require the establishment of a sustainable energy system. In this context, hydrogen (H_2) is considered as one of the most important and promising energy carriers for the decarbonization of key technologies and hereby allows achievement of the climate targets.[2–6] Hence, large-scale sustainable H_2 production processes are key on the way towards a modern hydrogen economy. In this regard, the pyrolysis of methane (CH_4) is a H_2 production route that requires significantly less energy than water electrolysis and, compared to state-of-the-art steam reforming, does not exhibit any direct carbon dioxide (CO_2) emissions.[3,7–10] CH_4 pyrolysis is an endothermic, thermal decomposition process during which gaseous H_2 and solid carbon are formed from CH_4 according to the global reaction eqn (1):[11–13]

$$CH_4 \rightarrow 2H_2 + C \quad \Delta_R H^\circ = 75\ \text{kJ mol}^{-1} \tag{1}$$

Despite the simple global reaction equation, the reaction mechanism comprising gas-phase chemistry as well as heterogeneous chemical reactions is extremely complex. It consists of a large number of elementary reactions that involve the coupling of CH_4 molecules to ethane and the subsequent step-wise dehydrogenation to ethylene and acetylene.[14–17] Further coupling of acetylene molecules results in the formation of benzene, which serves as an intermediate for polyaromatic hydrocarbons (PAHs). The latter can agglomerate to ultimately form elemental carbon in the form of soot and graphite.[18–22] Notably, the operation conditions strongly influence the nature, type, and morphology of the accrued carbon.[23] These carbon properties can be a decisive factor for the economic competitiveness of the pyrolysis process, which relies on a commercial usage of both gaseous hydrogen and solid carbon, *e.g.* in metallurgy or as a cathode material.[24,25]

The high stability of the CH_4 molecule results in a highly endothermic nature of the pyrolysis reaction.[26] Thus, temperatures between 500 °C and 1000 °C are needed to achieve technically relevant methane conversion rates and hydrogen yields even if catalytic systems, for example based on iron or nickel, are used.[27–30] The thermocatalytic pyrolysis of methane requires temperatures well above 1000 °C to activate the CH_4 molecule without a catalyst.[31] Despite the higher energy demand, thermocatalytic methane

---

Institute for Chemical Technology and Polymer Chemistry (ITCP), Karlsruhe Institute of Technology (KIT), Engesserstr. 20, 76131 Karlsruhe, Germany. E-mail: patrick.lott@kit.edu

† Electronic supplementary information (ESI) available. See DOI: **https://doi.org/10.1039/d3re00360d**

decomposition offers several advantages compared to catalytic processes relying on catalysts such as iron or nickel.[29,32] In particular, catalyst coking and impurities in the reactant stream that for instance may act as catalyst poison are essentially irrelevant. Hereby, longer and more stable operating times are achieved, and the resulting solid carbon can be extracted without any metallic impurities originating from a catalyst that may impede further usage.[32,33] CH_4 pyrolysis over carbon particles, which accelerate heterogeneous deposition reactions and provide additional surface area for particle growth, allows the above-mentioned advantages to be mostly maintained while lowering the temperature needed for a successful CH_4 decomposition.[32,34–39]

To date, fossil natural gas is the main source of CH_4 and therefore represents the main feedstock for methane pyrolysis processes. Although the pyrolytic conversion of natural gas extracts carbon from the gaseous energy carrier, the wide-spread usage of renewable methane sources rather than exploiting fossil sources would be much more elegant and desirable in the long term. Biogas obtained from the fermentation of biomass, for instance, is a promising alternative feedstock, but contains also up to almost 50% CO_2.[40] Under consideration of the harsh reaction conditions applied during the thermocatalytic pyrolysis of methane, additional reactions such as the dry reforming of methane (eqn (2)), the reverse water-gas shift (RWGS) reaction (eqn (3)), or the Boudouard reaction (eqn (4)) come into play.

$$CH_4 + CO_2 \rightleftharpoons 2CO + 2H_2 \quad \Delta_R H^\circ = 247\ \text{kJ mol}^{-1} \tag{2}$$

$$H_2 + CO_2 \rightleftharpoons CO + H_2O \quad \Delta_R H^\circ = 41\ \text{kJ mol}^{-1} \tag{3}$$

$$CO_2 + C \rightleftharpoons 2CO \quad \Delta_R H^\circ = 172\ \text{kJ mol}^{-1} \tag{4}$$

In all these reactions, the equilibrium for temperatures above 1000 °C is on the side of carbon monoxide (CO). Hence, in addition to the CH_4 conversion and the H_2 selectivity, the CO_2 conversion and the $H_2:CO$ ratio of the synthesis gas in the product stream are of particular interest.

Currently, pyrolysis processes enjoy great interest in academia and industry, especially in the context of chemical recycling and upcycling of carbonaceous materials and for energy generation. The potential impact on the environment is enormous: for example, waste from old fishing nets, wind turbine blades or conventional plastic waste can be converted to energy and high-value materials.[41–43] Herein, biomass or biowaste has also been considered as a feedstock.[44,45] However, even though some studies on the production of syngas or hydrogen from biomass or biogas have been conducted in the past,[6,46–51] the usage of biogas under reaction conditions of thermocatalytic pyrolysis of methane remains mostly unexplored. When the current political tensions in the energy market and fluctuating availability of resources are taken into account, flexible operation of methane pyrolysis with varying feed gas streams becomes a valuable asset to reliably meet the increasing demand for H_2 at all times. Most importantly, the use of biogas offers the potential for a negative carbon balance that actively reduces the greenhouse gas content in earth's atmosphere. In consideration of the overall biochemical process chain, namely CO_2 capture in biomass, fermentation of biomass to form biogas, and high-temperature pyrolysis to extract carbon and to form H_2, the carbon accrual during biogas pyrolysis can serve as a CO_2 sink.

By exposing CO_2-containing biogas as an alternative, sustainable CH_4 feedstock to thermocatalytic pyrolysis conditions in a lab-scale high-temperature reactor, this work systematically investigates the influence of temperature, residence time, H_2 dilution, and $CH_4:CO_2$ ratio in the biogas feed on CH_4 and CO_2 conversion as well as on H_2 and solid carbon yield. By comparing empty reactor tube experiments with results obtained when the reactor was loaded with a carbonaceous fixed bed, our study identifies advantageous operating parameters. Hereby, our work provides guidance for possible reactor configurations and operation conditions that can be used to design industrially viable full-scale processes.

Experimental

All experiments were conducted in an in-house developed high-temperature setup that was already described in previous publications.[14,52] The setup comprises a gas supply system, a reactor in plug-flow geometry, and an analysis and exhaust gas section as schematically depicted in Fig. 1a. By using mass flow controllers, a feed gas containing either pure methane or synthetic biogas, which is mixed from CH_4 and CO_2, was quantitatively fed and diluted with varying amounts of H_2. Subsequently, the reaction gas stream entered an electrically heated Al_2O_3-based ceramic reactor tube (DEGUSSIT AL23 by Friatec/Aliaxis) with an inner diameter of

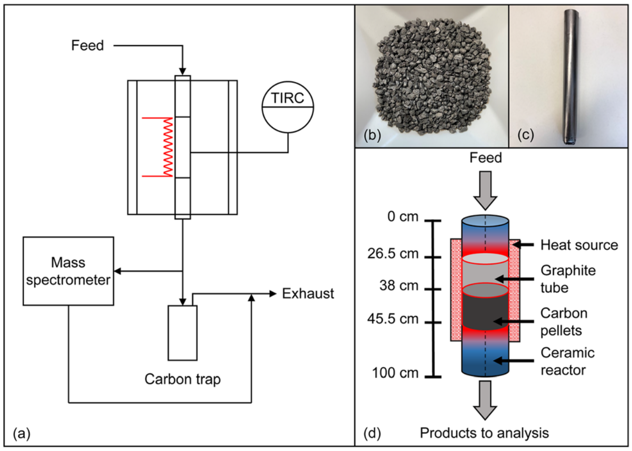

Fig. 1 Schematic flow diagram of the experimental setup (a), acetylene coke used as a base material of the fixed bed (b), a graphite container with flow holes at the bottom (c), and a scheme of the positioning of the carbon fixed bed container in the reactor (d).

20 mm. To ensure efficient insulation and safe reactor operation even in the case of over-pressure in the reactor tube, the reactor was located in a stainless-steel vessel. For accurate and continuous temperature measurement, a platinum-based thermocouple was used, which was positioned directly on the outer wall of the ceramic tube in the center of the heated reactor zone (Fig. 1a). Since solid particles form during the reaction, a trap was positioned downstream of the reactor for separation, and an additional particle filter was installed in order to remove fine soot particles. Finally, the effluent product gases are quantitatively analyzed in a Hiden Analytical HPR-20 R&D mass spectrometer. Details regarding data evaluation can be found in the ESI.†

In addition to experiments with an empty reactor tube, experiments with a carbonaceous fixed bed were conducted, for which 20 g of acetylene coke pellets (Carbolux, provided by BASF SE, Fig. 1b) with an average pellet diameter of 2 mm to 3 mm were filled into a 190 mm high container made of graphite foil (Fig. 1c). To ensure that the feed gas is heated to the respective reaction temperature before reaching the fixed bed, the container was positioned in the reactor so that the distance between the top of the fixed bed (length of 75 mm) and the reactor inlet was 380 mm (Fig. 1d). Note that a slight conical shape of the graphite container provided a seal at the top edge of the container and prevented bypass: the top seal forced the reaction gases to flow through the fixed bed, and the gases exited the fixed bed through holes at the bottom of the container (Fig. 1c).

The reactor was purged with argon (Ar) prior to each measurement and then continuously flushed with H_2 during the heating phase. During the experiments, the reactants were diluted with H_2. Although high H_2 levels were reported to inhibit CH_4 conversion,[53] the H_2 content is also a valuable parameter that can be used to control the formation of undesired byproducts, soot, and carbon deposits.[14] Hence, a carefully chosen H_2 dilution allows a fast pressure increase or even clogging of the reactor due to carbon deposition to be avoided. If not indicated otherwise, a molar H_2 : reaction gas ratio of 2 : 1 was chosen throughout this study, as this controls side-reactions to a certain extent while allowing a reasonable CH_4 conversion.

Once the desired reaction temperature was reached, the reactants diluted with H_2 were fed into the reactor for 20 minutes and the concentrations of the respective product gases were recorded with the mass spectrometer. Subsequently, the reactor was purged with Ar until all H_2 was removed and then carbonaceous deposits were burned off by flushing the reactor with synthetic air after each empty tube experiment. The burn-off was considered complete once no CO and CO_2 species in the exhaust gas were detected anymore. After another Ar purging phase to remove all oxygen from the reactor, the next experiment (20 min) with a new reaction gas mixture was conducted. In contrast, only one experiment was conducted if the reactor was loaded with a fixed bed and the reactor was cooled down to room temperature while purging with Ar, before the fixed bed could be removed.

Results and discussion

Following the aforementioned procedure, the influence of temperature (1000 °C, 1200 °C, 1400 °C, and 1600 °C), residence time (1 s, 3 s, 5 s, and 7 s), and biogas composition (molar $CH_4 : CO_2$ ratio 1 : 1, 2 : 1, and 4 : 1) was systematically investigated. In the focus were CH_4 and CO_2 conversion, H_2 selectivity, product composition, and solid carbon yield (definition of each is given in the ESI†). Note that the biogas compositions tested herein mimic typical $CH_4 : CO_2$ ratios as found for real-world biogas[40] and the set of reaction parameters applied throughout our experimental measurement campaign is based on previous studies that identified promising conditions for (industrially viable) H_2 production.[14,53] Furthermore, the effect of a carbonaceous fixed bed in the reactor was evaluated.

Influence of temperature

To investigate the effect of temperature on the reaction process in an empty reactor configuration, the temperature is varied when pyrolyzing either pure CH_4 or biogas with a molar $CH_4 : CO_2$ ratio of 2 : 1 in a gas mixture with a molar H_2 dilution ratio of 2 : 1 and a residence time of 5 s. Fig. 2 shows the CH_4 conversion (Fig. 2a) and H_2 selectivity (Fig. 2b) for both feeds during reactor operation at temperatures between 1000 °C and 1600 °C.

Irrespective of the feed gas composition, rising temperatures result in a significant increase in CH_4 conversion from approximately 20% at 1000 °C to almost 90% for pure CH_4 and more than 90% for biogas at 1400 °C; at 1600 °C, almost full conversion is achieved (Fig. 2a). Notably, the CH_4 conversion is higher when biogas is dosed, which can be attributed to a multitude of additional reaction pathways coming into play due to the presence of CO_2 (eqn (2)–(4)). This will be discussed in more detail below.

Although the temperature strongly influences the conversion, the H_2 selectivity (Fig. 2b) always exceeds 95% when pure CH_4 is used as a feed due to kinetic inhibition of most side reactions above 1000 °C.[53] Hence, the formation of byproducts hardly plays a role. For biogas as a feed, a rising reaction temperature promotes the H_2 selectivity, which is as high as 83% at 1000 °C and rises to 98% at 1400 °C. A further temperature increase to 1600 °C is only beneficial in terms of CH_4 conversion (Fig. 2a), but has only a marginal effect on the H_2 selectivity (Fig. 2b). The higher CH_4 conversion when using biogas as a feed may be due to a kinetic promotion of dry reforming (eqn (2)) at high temperatures. The lower H_2 selectivity for the biogas feed, however, may be due to a kinetic promotion of the RWGS reaction (eqn (3)).

Fig. 2c shows the product concentrations for a H_2/CH_4 gas feed. At 1000 °C, H_2 exhibits the highest share of approximately 74%, and unconverted methane with a

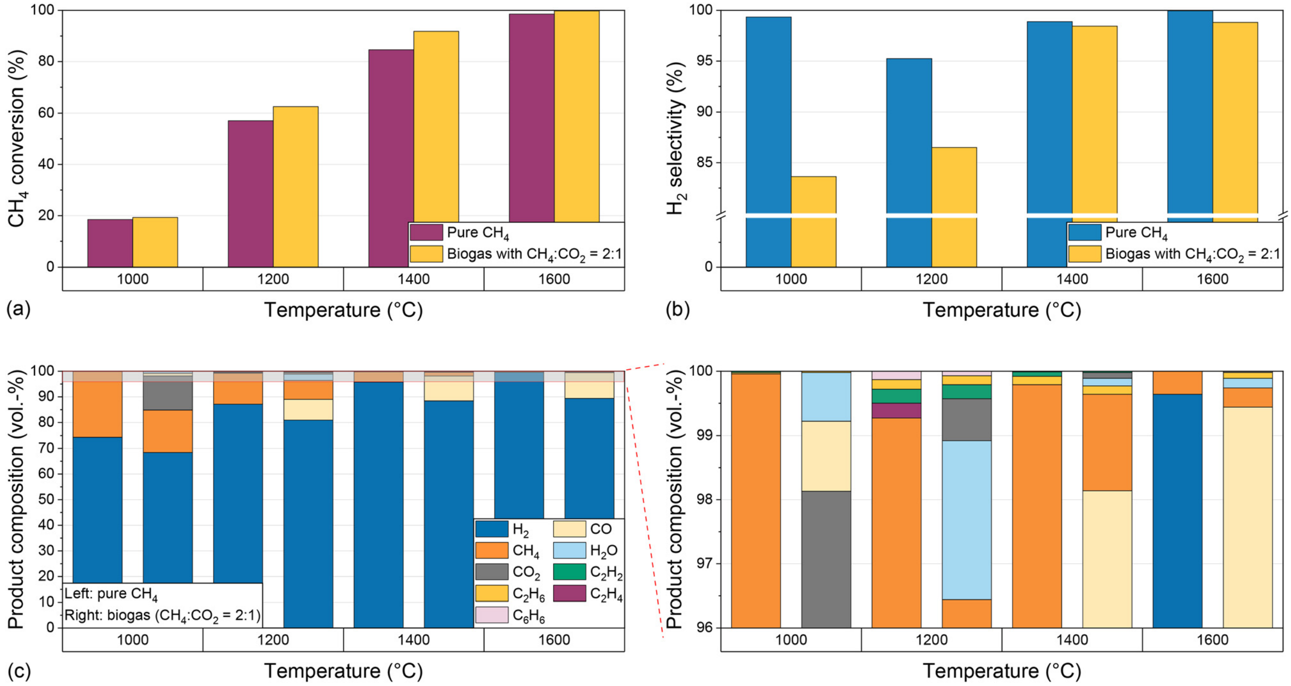

Fig. 2 Molar CH_4 conversion (a), molar H_2 selectivity (b), and product composition (c) for pure CH_4 and biogas ($CH_4:CO_2$ ratio 2 : 1) as a feed at temperatures from 1000 °C to 1600 °C, a residence time of 5 s, a molar $H_2:CH_4$ ratio of 2 : 1, and a molar H_2 : biogas ratio of 2 : 1.

volumetric share of approx. 25% is the predominant C-containing gas species. With increasing temperature, an increasing H_2 proportion and a decreasing methane content can be observed, corresponding to the increasing methane conversion and the comparably constant H_2 selectivity. Ethane (C_2H_6), ethylene (C_2H_4), acetylene (C_2H_2), and benzene (C_6H_6) can be identified as further byproducts. At 1000 °C and 1600 °C their total concentration is below 0.1%. At 1200 °C all four components mentioned above are formed in a concentration range between 0.1% and 0.2% each, and at 1400 °C only acetylene and ethane can be observed in a significant amount. The formation of these byproducts, which also play a role as essential intermediates during soot formation,[19] was also observed in previous studies at temperatures above 1000 °C.[53]

If biogas (CH_4/CO_2 diluted with H_2) is used as a feed, unreacted CO_2 can be observed in the product stream in addition to H_2 and unreacted CH_4. Its volume fraction drops from over 10% at 1000 °C to less than 1% at temperatures of 1200 °C and above (Fig. 2c). The decreasing CO_2 concentration correlates with the formation of CO, which is detected in significant amounts of up to 10% in the product gas stream at a temperature of 1200 °C and above, and whose origin we attribute to the dry reforming (eqn (2)) or the Boudouard reaction (eqn (4)). Furthermore, similar to experiments with a CH_4/H_2 feed gas, acetylene and ethane are formed in a significant amount, with volume fractions of 0.1% to 0.2% at 1200 °C and 1400 °C, which is significantly more than that at 1000 °C and 1600 °C. Last but not least, up to 2% of water (H_2O) is formed if the feed contains CO_2, which is due to the RWGS reaction (eqn (3)).

Influence of residence time and $CH_4:CO_2$ ratio

As previously mentioned, CO_2 can be consumed *via* dry reforming (eqn (2)) or *via* RWGS (eqn (3)), which both results in the formation of H_2 and CO. Since H_2/CO mixtures with various stoichiometries are widely used as syngas in industry, the $H_2:CO$ ratio in the effluent product gas stream is of particular importance. Fig. 3 shows CH_4 conversion (a), H_2 selectivity (b), and CO_2 conversion (c) for both H_2-diluted feeds, pure CH_4 and biogas, as a function of the residence time and $CH_4:CO_2$ ratio of the biogas at 1200 °C and 1400 °C.

The data point to a beneficial effect of an increasing residence time on CH_4 conversion, H_2 selectivity, and CO_2 conversion, although above 1400 °C residence time variations have a lower impact compared to temperatures as low as 1000 °C or 1200 °C. In analogy to previous findings on methane pyrolysis,[54] dry reforming,[55] and the RWGS reaction,[56] a longer exposure of the reactants to high temperatures enhances the thermocatalytic conversion of CH_4 and CO_2 and, in the case of CH_4, benefits the decomposition of intermediate species *via* dehydrogenation to form H_2 and solid carbon.[14] Moreover, the variations of the CO_2 content in the biogas mixtures uncovered that CH_4 conversion and H_2 selectivity increase with higher CH_4 content in the feed, but with a lower impact of the $CH_4:CO_2$ ratio at 1400 °C than at 1200 °C (Fig. 3a and b). Notably, the CO_2 conversion at 1400 °C exceeds 94% even under the most unfavorable conditions, namely a residence time of 1 s and a $CH_4:CO_2$ ratio of 1 : 1, and is higher for any other operational point (Fig. 3c). Even at 1200 °C, CO_2 conversion values of

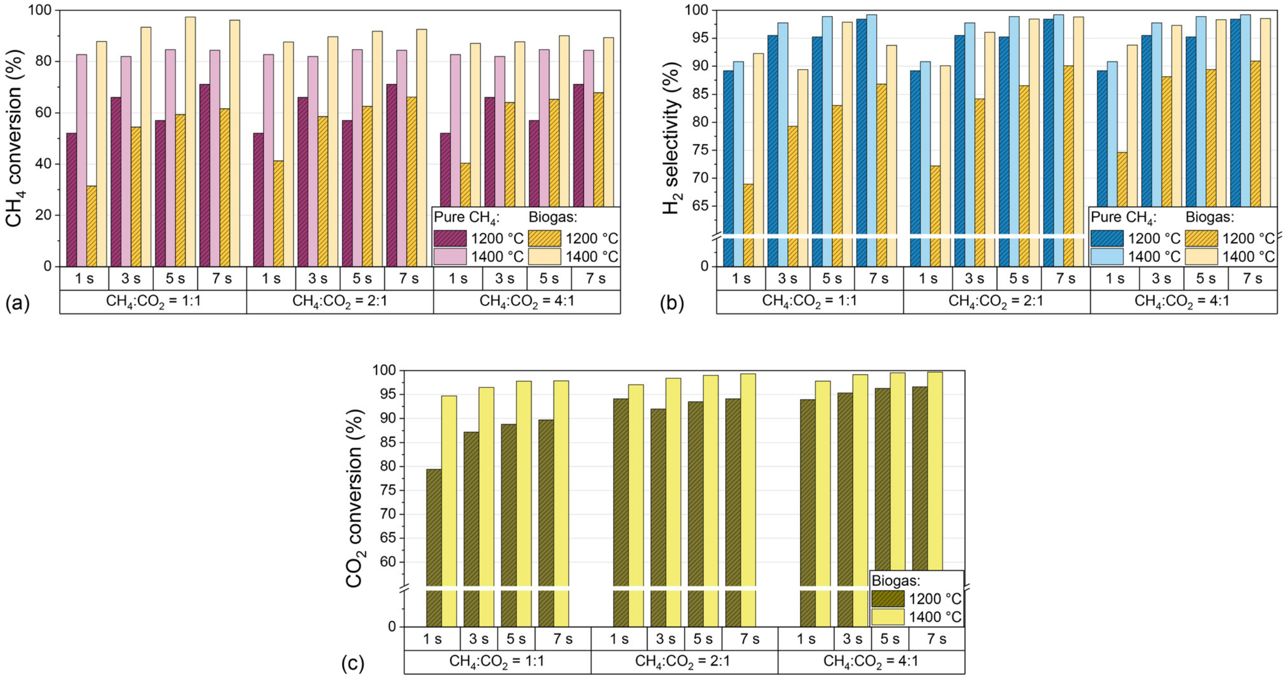

Fig. 3 Molar CH_4 conversion (a), molar H_2 selectivity (b), and molar CO_2 conversion (c) as a function of residence time and $CH_4:CO_2$ ratio of biogas at 1200 °C to 1400 °C, and a molar H_2 : biogas ratio of 2 : 1. As reference, data obtained with a feed gas that contains only CH_4 (in H_2 as a dilutant with a molar $H_2:CH_4$ ratio of 2 : 1) are also plotted in (a) and (b).

more than 95% can be achieved if the $CH_4:CO_2$ ratio is set to 4 : 1 and a residence time of 3 s or higher is chosen. These findings emphasize the huge potential of gas-phase biogas pyrolysis for efficient CO_2 transformation and utilization.

The substantial increase in CO_2 conversion with increasing temperature can be explained by the endothermicity of the equilibria. Furthermore, the conversion of CO_2 during dry reforming additionally promotes the

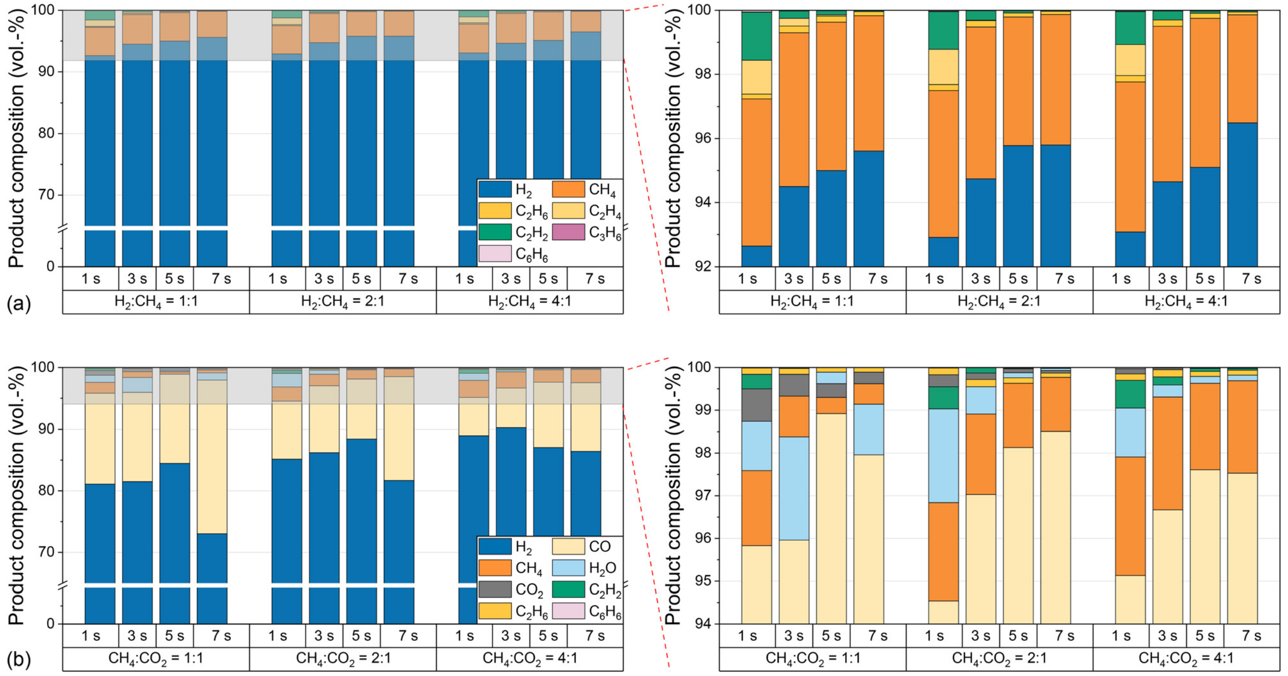

Fig. 4 Product composition for pure CH_4 (a) and biogas (b) as a function of residence time, molar $H_2:CH_4$ dilution, and molar $CH_4:CO_2$ ratio of biogas (in H_2 as a dilutant with a molar H_2 : biogas ratio of 2 : 1) at 1400 °C.

conversion of CH_4, which explains the higher CH_4 conversion in biogas feeds compared to measurements with pure CH_4. In contrast, the lower H_2 selectivity with biogas compared to measurements with pure CH_4 indicates a consumption of H_2, most likely *via* the RWGS reaction according to eqn (3), which also accounts for the formation of H_2O, *i.e.* as depicted in Fig. 4. In order to understand to what extent competing reactions influence the overall process, the product composition, in particular the CO concentration, must be examined in more detail. Hence, Fig. 4 shows the volume fractions of the product gas components when using either CH_4 only (a) or biogas (b) as the feed (both with H_2 dilution) at different residence times, $H_2:CH_4$ ratios, and biogas compositions at a temperature of 1400 °C.

With amounts of at least 92% in the product stream, H_2 is the main product when pure CH_4 is used in the feed, irrespective of the $H_2:CH_4$ ratio or the residence time; byproducts such as ethane, ethylene, acetylene, propylene or benzene form only to a small extent. These findings are consistent with previously postulated hydrocarbon decomposition mechanisms, where the aforementioned species act as intermediates for the formation of solid carbon.[14,19,37,38,57] Complementary to the CO_2 conversion data shown in Fig. 3c, only minor amounts of unconverted CO_2 are found in the effluent gas stream when using biogas as a feed (Fig. 4b). Instead, CO contents of up to 25% are found. Although some purification and process adaption may be necessary, for instance to remove humidity (H_2O contents of up to 2.5% are found, *cf.* Fig. 4b) or to tune the $H_2:CO$ ratio, the high CO content may allow a direct use of the effluent product gas stream as syngas. For instance, a $H_2:CO$ ratio of 1:1 is required for oxo synthesis or from 1:1 to 2:1 for the synthesis of alcohols.[58,59] Since H_2 serves as a diluent that is added to the feed gas stream, the reaction conditions subject to this work yield relatively H_2-rich syngas. As mentioned in the experimental part, dilution generally inhibits the formation of solids and unwanted byproducts. However, a dilution with H_2 in particular offers the advantage that no purification of the product gas is required afterwards, since it is part of the product itself. Note that the diluent H_2 from the feed is included in all figures showing product compositions. However, for the calculation of H_2 selectivity only the H_2 formed during the reaction was considered, as specified in the supporting information. In particular, the lowest $H_2:CO$ ratio of approximately 3:1 is observed at a temperature of 1400 °C when choosing a $CH_4:CO_2$ ratio of 1:1 and a residence time of 7 s. Since lower temperatures may result in syngas formation with lower $H_2:CO$ ratios, but at the expense of a drop in CH_4 and CO_2 conversion, downstream conditioning of the syngas would be more appropriate if lower $H_2:CO$ ratios are desired.[60]

In addition to CH_4 conversion, H_2 selectivity, and product gas composition, the amount of produced solid carbon in relation to the carbon entry in the form of CH_4 and CO_2 is of particular interest for an evaluation of the process with respect to its potential as a carbon sink. Thus, Fig. 5 shows the solid carbon yield as a function of residence time and $CH_4:CO_2$ ratio of the biogas at 1200 °C and 1400 °C; data for a feed gas stream containing only CH_4 diluted with H_2 are given as a reference. Note that the carbon amount was calculated from a carbon balance that includes all C-containing gas-phase species. PAHs that may deposit in minor quantity on the carbon accrued during methane pyrolysis[40,61] are not analyzed quantitatively. Hence, along with the uncertainty in gas-phase species quantification with the mass spectrometer, the minor yet unknown amount of PAHs contributes to the error bar. Generously estimated, we assume an error bar for the solid carbon yield data depicted in Fig. 5 of approx. 3% for experiments with pure CH_4. Since the experiments with biogas yield more different C-containing gas species with individual uncertainties in quantification, we assume a higher error of approx. 5%.

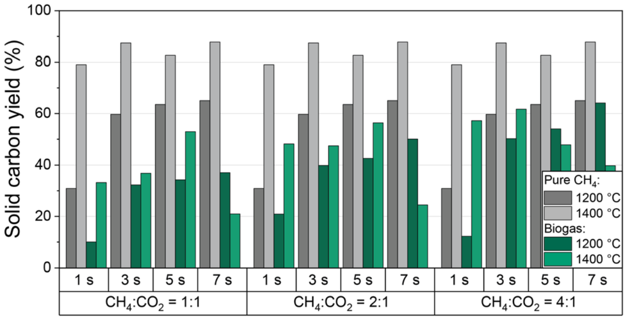

Fig. 5 Mass-based solid carbon yield as a function of residence time and molar $CH_4:CO_2$ ratio of biogas at 1200 °C to 1400 °C, and a molar H_2:biogas ratio of 2:1. As reference, data obtained with a feed gas that contains only CH_4 (in H_2 as a dilutant with a molar $H_2:CH_4$ ratio of 2:1) is also plotted.

For pure methane, the solid carbon yield is generally promoted either by increased temperature or residence time. A maximum carbon yield of almost 90% is found at a temperature of 1400 °C and a residence time of 7 s. These findings correlate well with the trends observed for methane conversion (Fig. 3a) that were already discussed above.

When feeding biogas, on the other hand, the carbon yield is always lower than for the feed gas with pure CH_4. Moreover, the solid carbon yield increases with an increasing proportion of methane in the feed gas, both at 1200 °C and 1400 °C. The maximum carbon yield of 65% was achieved at a $CH_4:CO_2$ ratio of 4:1, a residence time of 7 s, and a temperature of 1200 °C. A residence time-induced promotion of the solid carbon yield predominantly occurs at 1200 °C, whereas the solid carbon yield correlates directly with the volume fraction of CO in the product gas stream (Fig. 4b) at 1400 °C.

These observations indicate that in the case of a biogas feed the CH_4 molecules mainly participate in the pyrolysis reaction, while CO_2 primarily reacts in the reactions shown in eqn (2)–(4). Notably, in addition to CO_2, CH_4 is also consumed during dry reforming (eqn (2)), which increases the proportion of carbonaceous species that do not participate in the pyrolysis reaction, hereby decreasing the overall carbon yield.

In summary, the use of biogas offers the possibility of synthesis gas production and simultaneous fixation of a considerable proportion of carbon that enters the reactor *via* gas-phase species. Since the carbon produced during pyrolysis can also support the pyrolysis reaction,[14,62] the influence of a carbon-containing fixed bed is of particular interest and is therefore investigated in more detail in the following section.

Influence of a carbonaceous fixed bed

In addition to the process parameters that were already extensively discussed above, the introduction of carbon into the reactor, *e.g.* in the form of graphitic or amorphous carbon, can change the product composition.[32,39,62] As described in the experimental section, the reactor was loaded with a carbon particle fixed bed and its impact regarding CH_4 conversion (Fig. 6a), H_2 selectivity (Fig. 6b), and CO_2 conversion (Fig. 6c) was evaluated for H_2-diluted CH_4 and biogas feed streams. For this, the temperature and the $CH_4:CO_2$ ratio of the biogas were varied while keeping the residence time of 5 s and the H_2 dilution ratio of 2 : 1 constant.

The data depicted in Fig. 6 underscore that the introduction of a carbonaceous fixed bed significantly promotes CH_4 conversion (Fig. 6a) as well as H_2 selectivity (Fig. 6b), irrespective of the feed gas composition. At 1400 °C, both methane conversion and H_2 selectivity exceed 95%, with the highest CH_4 conversions observed when the feed gas contains biogas instead of only methane. On the other hand, the absence of CO_2 benefits the product selectivity towards H_2. With regard to the CO_2 conversion, the promoting effect of the carbonaceous fixed bed depends on the $CH_4:CO_2$ ratio and the temperature. In particular, the fixed bed increases the CO_2 conversion from 87% to 97% at a $CH_4:CO_2$ ratio of 1 : 1 and a temperature of 1200 °C. However, the promoting effect decreases with increasing temperature and $CH_4:CO_2$ ratio and is almost negligible at a $CH_4:CO_2$ ratio of 4 : 1.

Our results with a feed gas that contains only (H_2-diluted) CH_4 underscore the beneficial effect of carbon on methane pyrolysis, which is in accordance with previous findings.[14,34,36,62] In this context, the catalytic effect of carbon is particularly dependent on structural and surface properties. It is assumed that surface defects, or more precisely high-energy sites of the carbon surface, are capable of activating the methane molecule.[39] These defects are found primarily in disordered, amorphous materials, such as the acetylene coke used in this work.

More importantly, our experiments with a biogas feed stream suggest that a carbonaceous fixed bed is not only beneficial for CH_4 conversion and H_2 selectivity, but also enhances CO_2 conversion as uncovered by the results presented in Fig. 6c. At all temperatures and $CH_4:CO_2$ ratios, the fixed bed promotes the conversion of CO_2. While the conversion increase is most pronounced for the experiments with high CO_2 content in the feed gas and at 1200 °C, the difference between the results for an empty reactor and a fixed bed configuration becomes smaller with rising CH_4

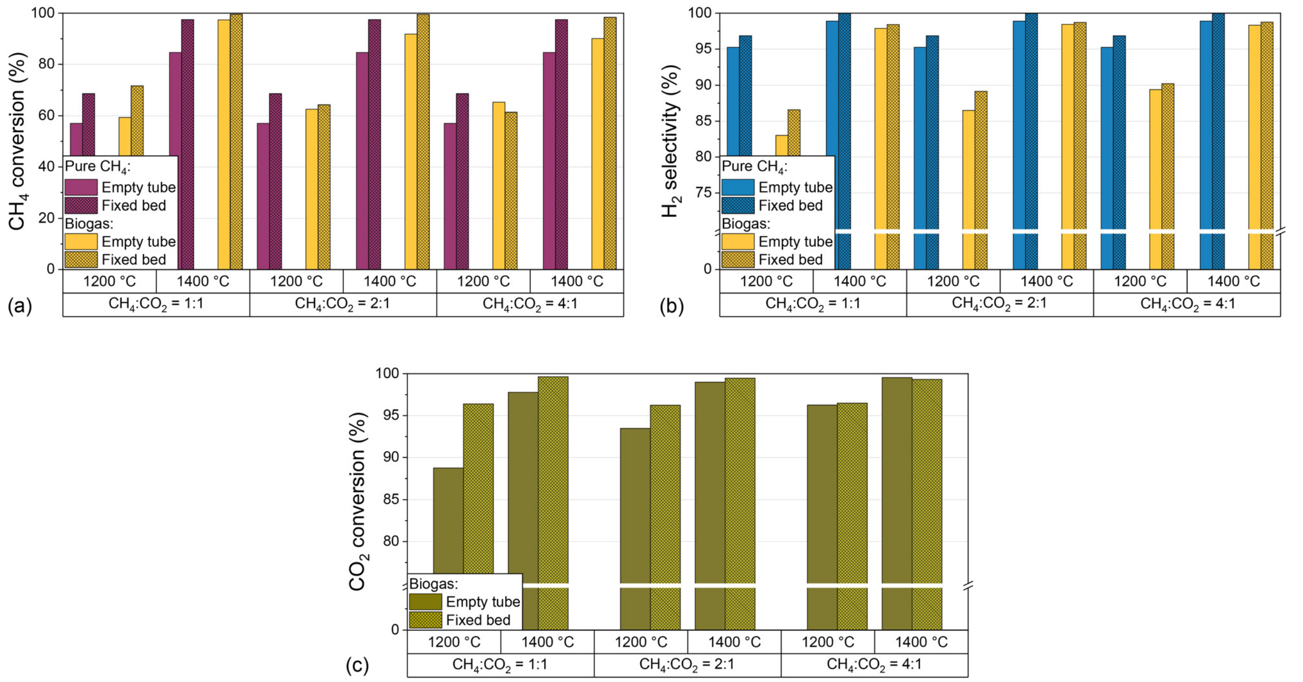

Fig. 6 Empty tube and fixed bed results for molar CH_4 conversion (a), molar H_2 selectivity (b) for pure CH_4 and biogas and molar CO_2 conversion (c) for biogas as a function of temperature and molar $CH_4:CO_2$ ratio of biogas at a constant residence time of 5 s and a molar H_2 dilution ratio of 2 : 1.

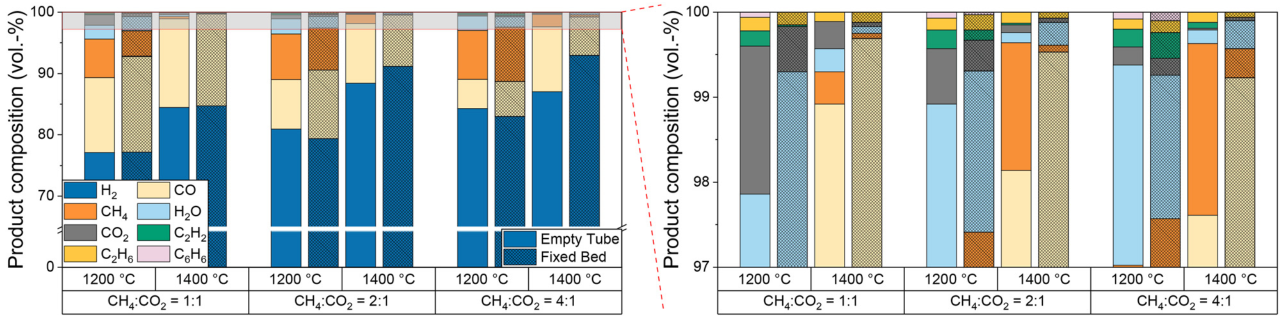

Fig. 7 Empty tube and fixed bed results for product composition for biogas as a function of temperature and molar $CH_4:CO_2$ ratio of biogas at a constant residence time of 5 s and a molar H_2 dilution ratio of 2 : 1.

content and at 1400 °C. We attribute this converging behavior to a promotion of the forward reactions of eqn (2)–(4) in gas compositions with high CO_2 contents, both due to the endothermic nature of these reactions and Le Chatelier's principle.[63–65]

Furthermore, since the product stream composition is a key parameter for understanding and optimizing the overall process, especially when using biogas as a feed, Fig. 7 provides further details on the product gas composition as a function of temperature and $CH_4:CO_2$ ratio. Compared to empty tube tests, the introduction of a carbonaceous fixed bed does not only decrease the CH_4 and CO_2 concentrations in the effluent gas stream, especially at a temperature of 1400 °C, but also suppresses the formation of the byproducts ethane, acetylene, benzene, and water.

At a $CH_4:CO_2$ ratio of 1 : 1, our data suggest that the use of a fixed bed mainly promotes CO formation. Although the H_2 content in the product gas stream is almost the same, a lower methane content is found in the product gas stream compared to the empty reactor experiments. This composition of the product gas stream indicates that dry reforming (eqn (2)) consumes methane and carbon dioxide over a carbonaceous fixed bed, resulting in the formation of CO and H_2. As suggested by the H_2O content in the product gas stream, the reverse water-gas shift reaction (eqn (3)) converts considerable amounts of H_2 and CO_2 into CO and H_2O at 1200 °C. This observation matches with the equilibrium constant of the RWGS reaction at temperatures above 1100 °C.[56] Despite its endothermic nature, RWGS seems to become significantly less relevant at 1400 °C, as less steam is observed in the effluent gas stream. This apparent mismatch may be explained by a reaction between H_2O and CH_4 to form CO (or CO_2) and H_2, which is essentially a reverse methanation reaction. As methanation itself is strongly exothermic, temperatures above 700 °C promote the reverse reaction.[66] However, since a lower methane content is always accompanied by a higher H_2 content due to the pyrolysis reaction itself although a possible *in situ* consumption of H_2O formed *via* the RWGS reaction would result in a comparably lower H_2 evolution, more detailed experiments are necessary to uncover the mechanistic details in the future. An increasing $CH_4:CO_2$ ratio (namely 2 : 1 and 4 : 1) diminishes the effect of the fixed bed on the methane content, but still a beneficial effect on the CO_2 conversion remains. The higher CO content found during experiments with the fixed bed reactor configuration is desirable when the product stream is supposed to be used as syngas.

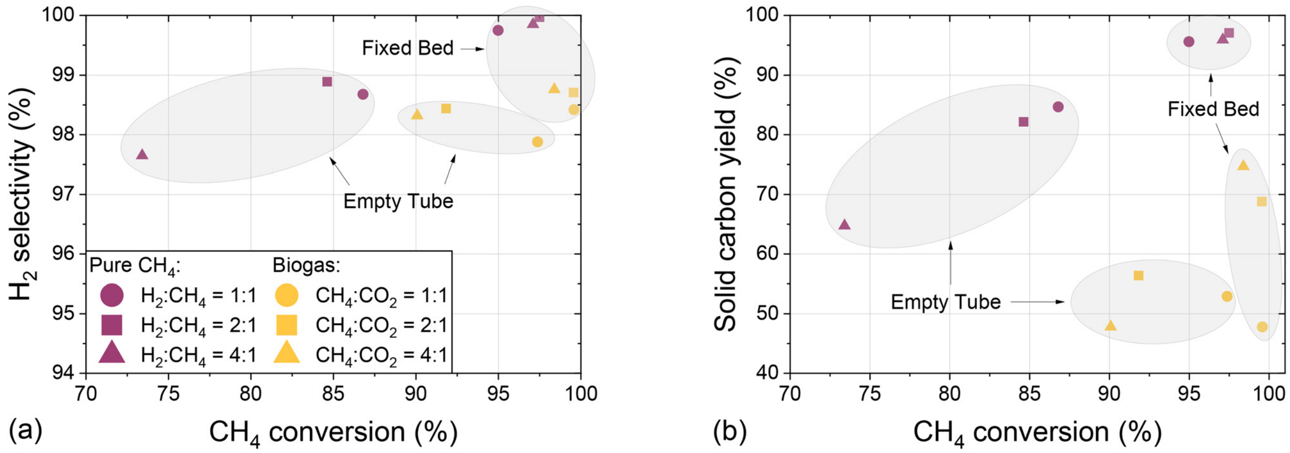

Fig. 8 Molar H_2 selectivity (a) and mass-based solid carbon yield (b) as a function of molar CH_4 conversion for pure CH_4 and biogas feeds in an empty tube and fixed bed configuration at a temperature of 1400 °C, a residence time of 5 s, and a constant molar H_2 : biogas ratio of 2 : 1.

In order to assess the suitability of methane and biogas pyrolysis as a process acting as a carbon sink, Fig. 8 summarizes experiments conducted with an empty tube and a fixed bed reactor configuration by showing the H_2 selectivity (Fig. 8a) and the solid carbon yield (Fig. 8b) as a function of CH_4 conversion and with varying H_2 dilution.

The data presented in Fig. 8a clearly emphasize that the use of a fixed bed increases both methane conversion and H_2 selectivity, irrespective of the $H_2:CH_4$ dilution ratio and biogas composition. Compared to experiments with pure methane, the use of CO_2-containing biogas barely reduces the selectivity towards hydrogen and allows for even higher methane conversion. These observations underscore the flexibility of the studied pyrolysis process in terms of feed gas composition. Similarly, the data presented in Fig. 8b reveal that the use of a carbonaceous fixed bed benefits the formation of solid elemental carbon not only in a feed gas containing solely CH_4, but also in a biogas-based feed stream. The feed with a $CH_4:CO_2$ ratio of 1:1 is the only exception, which we assume is due to the high CO_2 content that benefits the Boudouard reaction (eqn (4)). For both reactor configurations, the carbon yields for experiments with pure methane as a feed always exceed those for experiments with a biogas feedstock. This observation substantiates the above-mentioned hypothesis that it is primarily the carbon from the methane molecules in the feed gas that can be fixed in solid form, whereas CO_2 is rather reacting to CO. Since under the conditions subject to the present study the carbon yield in a fixed bed reactor configuration varies between 47% and 75% when using biogas, corresponding to $CH_4:CO_2$ ratios of 1:1 and 4:1, respectively, pyrolysis is an auspicious process for carbon fixation in elemental solid carbon. Non-solid carbon is predominantly bound in CO, which along with H_2 in the product gas stream can serve as synthesis gas.

Conclusions

Our work that was conducted in a lab-scale high-temperature pyrolysis reactor evaluates the thermocatalytic decomposition of biogas at high temperatures and compares the results with results obtained for conventional CH_4 pyrolysis. Hereby, we analyze the suitability of biogas pyrolysis for H_2 and syngas production and simultaneous carbon capture. Our tests identified the main reaction parameters that govern CH_4 conversion, H_2 selectivity, CO_2 conversion, and product composition, namely temperature, residence time, H_2 content in the feed gas, and the molar $CH_4:CO_2$ ratio of the biogas used as a feedstock.

For H_2-diluted feed gas streams containing either pure CH_4 or biogas, CH_4 conversions, H_2 selectivities, and CO_2 conversions of more than 90% are achieved at temperatures of 1400 °C and above. Herein, an increase of the residence time from 1 s to 7 s does not only promote the conversion of CH_4 and CO_2, but also enhances the selectivity to H_2. Moreover, a high CH_4 content and low amounts of CO_2 in the feed promote CH_4 conversion and H_2 selectivity especially at temperatures as low as 1200 °C, whereas the impact of the $CH_4:CO_2$ ratio diminishes at temperatures of 1400 °C and above. Although without doubt higher temperatures further increase operating costs, they also allow the process to be operated with higher H_2 dilutions while still maintaining a sufficiently high CH_4 conversion. In terms of process design, a high H_2 dilution is very attractive as it ensures a safe operation with reduced byproduct formation and improved control of the solid formation, hereby resulting in less reactor clogging.

In addition to the primary product H_2, the usage of biogas as a feed results in considerable CO formation; reactor operation at 1400 °C, a residence time of 7 s, and a $CH_4:CO_2$ ratio of 1:1 yields the highest CO content and results in a $H_2:CO$ ratio of approximately 3:1. Although the product gas stream can be used directly as syngas, a further tuning of the $H_2:CO$ ratio may be mandatory in order to account for downstream follow-up processes. For instance, if lower $H_2:CO$ ratios are needed, lower temperatures could be used, however, at the expense of CH_4 and CO_2 conversion. Although the design of a real-world process would require a profound techno-economic analysis, downstream conditioning of the syngas could be more appropriate, considering the trade-off between feed stream conversion and product stream composition.

Moreover, the formation of solid carbon is promoted by high temperatures and high residence time. At a temperature of 1400 °C and a residence time of 7 s, a solid carbon yield of almost 90% is achieved when using pure methane as a feed gas. When using biogas instead, high methane contents in the feed promote the formation of elemental carbon with a maximum carbon yield of 65% at a $CH_4:CO_2$ ratio of 4:1, a residence time of 7 s, and a temperature of 1200 °C. Herein, the solid carbon yield directly correlates with the volume fraction of CO in the product gas stream, indicating that mainly the methane molecules participate in the pyrolysis reaction, whereas CO_2 is predominantly converted to CO *via* dry reforming and reverse water-gas shift reactions.

Finally yet importantly, the presence of a carbonaceous fixed bed enhances heterogeneous reactions during carbon deposition, hereby promoting the conversion of both CH_4 and CO_2, increasing the selectivity to H_2, and suppressing the formation of undesired byproducts such as ethane, ethylene, or benzene. In addition, the fixed bed promotes the yield of solid carbon, allowing a carbon fixation of up to 95% for a feed gas stream containing pure CH_4 to be achieved. When using biogas as a feedstock, the carbon yield directly correlates with the methane content in the feed, which can be attributed to the pyrolytic reaction pathways for CH_4 and the dry reforming and reverse water-gas shift reactions consuming CO_2. Remarkably, at a temperature of 1400 °C and a residence time of 5 s, the solid carbon yield in a biogas-based feed with a $CH_4:CO_2$ ratio of 4:1 is as high as 75%, which is an encouraging value regarding carbon capture and simultaneous syngas production without any direct CO_2 emissions.

In addition, the use of comparably cheap carbon as the material for the fixed bed suggests a high economic appeal, particularly considering that metal impurities in the deposited carbon are irrelevant, which otherwise cannot be avoided if conventional metal-based catalysts are used for CH_4 and CO_2 activation. Beyond a simple sequestration of accrued carbon, the commercialization of the solid carbon product is considered essential for establishing an economically competitive process.[7] Hence, further characterization, especially in terms of structural parameters or particle size distribution as a function of the operational points, is imperative. In addition to a detailed deconvolution of competing reaction pathways in the gas-phase, *i.e.* pyrolysis, dry reforming, reverse water-gas shift, and the Boudouard reaction, future studies also need to clarify whether the presence of oxygen-containing species such as CO_2 has an impact on the accrued carbon and therefore on its further usage.

Conflicts of interest

There are no conflicts to declare.

Acknowledgements

We thank M. Bender J. Bode, K. Ehrhardt, D. Flick, F. Scheiff, and D. Schlereth (BASF) for fruitful discussions, M. Berg and C. Kroll (Berg-idl GmbH) for their support in engineering the high-temperature vessel of the experimental setup, and S. Lichtenberg (KIT) for technical support.

Notes and references

1 C. A. Horowitz, *International Legal Materials*, 2016, **55**, 740–755.
2 M. van der Spek, C. Banet, C. Bauer, P. Gabrielli, W. Goldthorpe, M. Mazzotti, S. T. Munkejord, N. A. Røkke, N. Shah, N. Sunny, D. Sutter, J. M. Trusler and M. Gazzani, *Energy Environ. Sci.*, 2022, **15**, 1034–1077.
3 O. Machhammer, A. Bode and W. Hormuth, *Chem. Eng. Technol.*, 2016, **39**, 1185–1193.
4 V. M. Maestre, A. Ortiz and I. Ortiz, *Renewable Sustainable Energy Rev.*, 2021, **152**, 111628.
5 S. Griffiths, B. K. Sovacool, J. Kim, M. Bazilian and J. M. Uratani, *Energy Res. Soc. Sci.*, 2021, **80**, 102208.
6 P. Lott and O. Deutschmann, *Proc. Combust. Inst.*, 2023, **39**, 3183–3215.
7 B. Parkinson, P. Balcombe, J. F. Speirs, A. D. Hawkes and K. Hellgardt, *Energy Environ. Sci.*, 2019, **12**, 19–40.
8 K. Christopher and R. Dimitrios, *Energy Environ. Sci.*, 2012, **5**, 6640–6651.
9 N. Sánchez-Bastardo, R. Schlögl and H. Ruland, *Ind. Eng. Chem. Res.*, 2021, **60**, 11855–11881.
10 S. Schneider, S. Bajohr, F. Graf and T. Kolb, *ChemBioEng Rev.*, 2020, **7**, 150–158.
11 N. Muradov and T. Veziroğlu, *Int. J. Hydrogen Energy*, 2005, **30**, 225–237.
12 H. F. Abbas and W. Wan Daud, *Int. J. Hydrogen Energy*, 2010, **35**, 1160–1190.
13 U. Ashik, W. Wan Daud and H. F. Abbas, *Renewable Sustainable Energy Rev.*, 2015, **44**, 221–256.
14 P. Lott, M. B. Mokashi, H. Müller, D. J. Heitlinger, S. Lichtenberg, A. B. Shirsath, C. Janzer, S. Tischer, L. Maier and O. Deutschmann, *ChemSusChem*, 2023, **16**, e202201720.
15 G. Fau, N. Gascoin, P. Gillard and J. Steelant, *J. Anal. Appl. Pyrolysis*, 2013, **104**, 1–9.
16 C.-J. Chen, M. H. Back and R. A. Back, in *Industrial and Laboratory Pyrolyses*, ed. L. F. Albright and B. L. Crynes, American Chemical Society, 1976, pp. 1–16.
17 A. Holmen, O. Olsvik and O. A. Rokstad, *Fuel Process. Technol.*, 1995, **42**, 249–267.
18 W. Benzinger, A. Becker and K. J. Hüttinger, *Carbon*, 1996, **34**, 957–966.
19 J. Appel, H. Bockhorn and M. Frenklach, *Combust. Flame*, 2000, **121**, 122–136.
20 A. B. Shirsath, M. Mokashi, P. Lott, H. Müller, R. Pashminehazar, T. Sheppard, S. Tischer, L. Maier, J.-D. Grunwaldt and O. Deutschmann, *J. Phys. Chem. A*, 2023, **127**, 2136–2147.
21 M. R. Kholghy, G. A. Kelesidis and S. E. Pratsinis, *Phys. Chem. Chem. Phys.*, 2018, **20**, 10926–10938.
22 M. Frenklach, *Symp. (Int.) Combust., [Proc.]*, 1996, **26**, 2285–2293.
23 A. Böttcher, F. Hennrich, H. Rösner, S. Malik, M. M. Kappes, S. Lichtenberg, G. Schoch and O. Deutschmann, *Carbon*, 2007, **45**, 1085–1096.
24 T. I. Korányi, M. Németh, A. Beck and A. Horváth, *Energies*, 2022, **15**, 6342.
25 S. Timmerberg, M. Kaltschmitt and M. Finkbeiner, *Energy Convers. Manage.: X*, 2020, **7**, 100043.
26 N. Muradov, F. Smith, C. Huang and A. T. Raissi, *Catal. Today*, 2006, **116**, 281–288.
27 L. Zhou, L. R. Enakonda, M. Harb, Y. Saih, A. Aguilar-Tapia, S. Ould-Chikh, J.-L. Hazemann, J. Li, N. Wei, D. Gary, P. Del-Gallo and J. Basset, *Appl. Catal., B*, 2017, **208**, 44–59.
28 S. H. Sharif Zein, A. R. Mohamed and P. S. Talpa Sai, *Ind. Eng. Chem. Res.*, 2004, **43**, 4864–4870.
29 N. Muradov, *Energy Fuels*, 1998, **12**, 41–48.
30 T. Keipi, K. E. Tolvanen, H. Tolvanen and J. Konttinen, *Energy Convers. Manage.*, 2016, **126**, 923–934.
31 A. Abánades, E. Ruiz, E. M. Ferruelo, F. Hernández, A. Cabanillas, J. M. Martínez-Val, J. A. Rubio, C. López, R. Gavela, G. Barrera, C. Rubbia, D. Salmieri, E. Rodilla and D. Gutiérrez, *Int. J. Hydrogen Energy*, 2011, **36**, 12877–12886.
32 N. Muradov, *Catal. Commun.*, 2001, **2**, 89–94.
33 D. P. Serrano, J. A. Botas and R. Guil-Lopez, *Int. J. Hydrogen Energy*, 2009, **34**, 4488–4494.
34 D. P. Serrano, J. Botas, P. Pizarro and G. Gómez-Pozuelo, *Int. J. Hydrogen Energy*, 2013, **38**, 5671–5683.
35 D. P. Serrano, J. A. Botas, J. Fierro, R. Guil-López, P. Pizarro and G. Gómez, *Fuel*, 2010, **89**, 1241–1248.

36 J. Zhang, X. Li, H. Chen, M. Qi, G. Zhang, H. Hu and X. Ma, *Int. J. Hydrogen Energy*, 2017, **42**, 19755–19775.

37 K. Norinaga and O. Deutschmann, *Ind. Eng. Chem. Res.*, 2007, **46**, 3547–3557.

38 K. Norinaga, O. Deutschmann, N. Saegusa and J.-I. Hayashi, *J. Anal. Appl. Pyrolysis*, 2009, **86**, 148–160.

39 N. Muradov, F. Smith and A. T. Raissi, *Catal. Today*, 2005, **102**, 225–233.

40 A. Calbry-Muzyka, H. Madi, F. Rüsch-Pfund, M. Gandiglio and S. Biollaz, *Renewable Energy*, 2022, **181**, 1000–1007.

41 S. Kim, Y. T. Kim, L. S. Oh, H. J. Kim and J. Lee, *J. Mater. Chem. A*, 2022, **10**, 20024–20034.

42 W. Yang, K.-H. Kim and J. Lee, *J. Cleaner Prod.*, 2022, **376**, 134292.

43 C. Park, H. Lee, N. Lee, B. Ahn and J. Lee, *J. Hazard. Mater.*, 2022, **440**, 129825.

44 J. Kim, C. Park, H. Park, J. Han, J. Lee and S.-K. Kim, *Energy*, 2022, **258**, 124877.

45 H. Park, J. Joo, J. Kim, J. Lee and S.-K. Kim, *Energy*, 2023, **278**, 127797.

46 C. H. Geissler and C. T. Maravelias, *Energy Environ. Sci.*, 2022, **15**, 2679–2689.

47 H. Liu, N. Agrawal, A. Ganguly, Y. Chen, J. Lee, J. Yu, W. Huang, M. Mba Wright, M. J. Janik and W. Li, *Energy Environ. Sci.*, 2022, **15**, 4175–4189.

48 R. M. Navarro, M. C. Sánchez-Sánchez, M. C. Alvarez-Galvan, F. Del Valle and J. L. G. Fierro, *Energy Environ. Sci.*, 2009, **2**, 35–54.

49 X. Zhao, B. Joseph, J. Kuhn and S. Ozcan, *iScience*, 2020, **23**, 101082.

50 R. Sivaranjani, S. Veerathai, K. Jeoly Jenifer, K. Sowmiya, K. J. Rupesh, S. Sudalai and A. Arumugam, *Int. J. Hydrogen Energy*, 2023, **48**, 23785–23820.

51 M. Ni, D. Y. Leung, M. K. Leung and K. Sumathy, *Fuel Process. Technol.*, 2006, **87**, 461–472.

52 S. D. Angeli, S. Gossler, S. Lichtenberg, G. Kass, A. K. Agrawal, M. Valerius, K. P. Kinzel and O. Deutschmann, *Angew. Chem.*, 2021, **60**, 11852–11857.

53 C. Guéret, M. Daroux and F. Billaud, *Chem. Eng. Sci.*, 1997, **52**, 815–827.

54 O. Olsvik, O. A. Rokstad and A. Holmen, *Chem. Eng. Technol.*, 1995, **18**, 349–358.

55 U. Olsbye, T. Wurzel and L. Mleczko, *Ind. Eng. Chem. Res.*, 1997, **36**, 5180–5188.

56 F. Bustamante, R. M. Enick, A. V. Cugini, R. P. Killmeyer, B. H. Howard, K. S. Rothenberger, M. V. Ciocco, B. D. Morreale, S. Chattopadhyay and S. Shi, *AIChE J.*, 2004, **50**, 1028–1041.

57 M. Frenklach, *Phys. Chem. Chem. Phys.*, 2002, **4**, 2028–2037.

58 H. Weber and J. Falbe, *Ind. Eng. Chem.*, 1970, **62**, 33–37.

59 H. T. Luk, C. Mondelli, D. C. Ferré, J. A. Stewart and J. Pérez-Ramírez, *Chem. Soc. Rev.*, 2017, **46**, 1358–1426.

60 M. M. Yung, W. S. Jablonski and K. A. Magrini-Bair, *Energy Fuels*, 2009, **23**, 1874–1887.

61 G. F. Glasier, R. Filfil and P. D. Pacey, *Carbon*, 2001, **39**, 497–506.

62 V. Shilapuram, N. Ozalp, M. Oschatz, L. Borchardt and S. Kaskel, *Carbon*, 2014, **67**, 377–389.

63 M. Jafarbegloo, A. Tarlani, A. W. Mesbah and S. Sahebdelfar, *Int. J. Hydrogen Energy*, 2015, **40**, 2445–2451.

64 M. Wenzel, L. Rihko-Struckmann and K. Sundmacher, *AIChE J.*, 2017, **63**, 15–22.

65 P. Lahijani, Z. A. Zainal, M. Mohammadi and A. R. Mohamed, *Renewable Sustainable Energy Rev.*, 2015, **41**, 615–632.

66 J. Gao, Y. Wang, Y. Ping, D. Hu, G. Xu, F. Gu and F. Su, *RSC Adv.*, 2012, **2**, 2358–2368.